Is Ductile Cast Iron Ductile at -40°C ?

N. Urabe [1] *and K. Furuta* [2]

[1] Steel Research Center, NKK Corporation, Kawasaki-city, Japan
[2] Engineering Department, NKK Corporation, Yokohama-city, Japan

INTRODUCTION

Casks for transportation and storage of spent nuclear fuels, fabricated from ductile cast iron (DCI) have now attracted strong interest in Japan, with considerable effort expended toward their application. Such casks must maintain their structural integrity even when subjected to hypothetical accidents during transport to or handling at storage facilities. The International Atomic Energy Agency (IAEA) standards (IAEA 1985) require that type B casks, for instance, withstand a nine-meter free drop onto an unyielding target at a lowest service temperature of -40°C, and they retain sufficient shielding efficiency. Such loading conditions envelope severe transportation collision accidents. Heavy-section DCI casks, with wall thicknesses of the order of 400mm, would be suspected to undergo a ductile-to-brittle transition that is a function of temperature and loading rate. Mechanical properties and fracture toughness at low service temperatures, under impact loading conditions, therefore, must be estimated accurately to assure the ductile behavior.

Torsion tests and fracture toughness (initiation and arrest) tests were carried out on samples extracted from a prototypic cask and two model casks fabricated from ductile cast iron, to confirm that ductile cast iron has sufficient ductility and fracture toughness even at low temperatures and under tri-axial stress state conditions.

For the assessment of the structural integrity of cask, a linear elastic fracture mechanics approach is appropriate. The integrity of the cask should be assured so that the brittle failure never takes place even if a crack-like flaw of fairly large size associated with detection sensitivity of non-destructive tests is postulated in the cask. Examples of safety analysis on the cask were also carried out based on a linear elastic fracture mechanics approach.

DUCTILE CAST IRON CASKS AND EXTRACTION OF TEST PIECES

A prototypic cask (outer diameter=2222mm, wall thickness=360mm, length=5000mm), a model cask S (od=2222mm, t=360mm, *l*=3000mm) and a model cask H (od=2300mm, t=400mm, *l*=2130mm) cast by hot direct founding method (Yamase et al. 1987) were used to examine the ductility and the fracture toughness of heavy-section ductile cast iron (ASTM A874: ASTM 1989 or JIS G4405: JIS 1992). The details of the cask production process and fundamental physical, metallurgical and mechanical properties are shown elsewhere (Urabe and Harada 1989, Harada and Urabe 1989).

Several blocks were cut out along the longitudinal direction of casks, then test specimens were machined from each block. Torsion test specimens were cut out so that the gauge length is 150mm, the diameter is 15mm and the overall length is 400mm. For the initiation fracture toughness tests, six inch thick compact tension (6TCT, 150mm thick) specimens and eight inch thick compact tension (8TCT, 200mm thick) specimens were machined in conformity with ASTM E399 test methods (ASTM 1990). In some of the specimens, side-face grooves (25% deep, 45° flank angle, 0.25mm tip radius) were machined to increase the mechanical constraint condition. Side grooved 6TCT specimens with varying thickness (50mm ~ 100mm) were also machined to measure the arrest fracture toughness.

TORSION TESTS

Torsion tests were carried out at 18°C and -40°C under different strain rates. Examples of shear stress-shear strain records are shown in Fig. 1. The shear stress in the plastically deformed region increases with the increase in strain rate and decreases in temperature. It is also seen in the stress-strain records that DCI does not exhibit distinct yield phenomena as the tensile stress-strain curve does not. Thus, the yield stress of torsion tests was determined with an analogy to 0.2% proof stress in tension tests. According to an elastic calculation, the shear strain corresponding to 0.2% tensile strain can be obtained as 0.26 or 0.3% if the yielding condition of DCI obeys either Tresca's criterion ($\tau_Y/\sigma_Y=1/2$) or von Mises and Henckey's criterion ($\tau_Y/\sigma_Y=1/\sqrt{3}$).

$$\gamma_Y/\varepsilon_Y=(\tau_Y/G)/(\sigma_Y/E)=2(1+\nu)\cdot(\tau_Y/\sigma_Y) \approx 1.3 \sim 1.5 \qquad (1)$$

where γ and ε are shear strain and tensile strain, τ and σ are shear stress and tensile stress, G and E are shear modulus and Young's modulus, ν is Poisson's ratio and subscript Y stands for the yielding.

The calculated shear yield stress is shown in Table 1. The yield stress, $\tau_{0.3}$, corresponding to the offset of 0.3% shear strain is about 160N/mm^2 for ambient temperature (18°C) and 180 ~ 190 N/mm^2 for -40°C. The shear strain at the onset of failure, γ_B, is about 100% at 18°C and 60 ~ 90% at -40°C. Photo 1 shows examples of scanning electron micrograph of fractured surface. It can be seen in Photo 1 (a) that ferritic matrix around graphite particles was severely deformed and finally slipped off as the results of void nucleation and coalescence that is a typical ductile deformation and failure process. Another example of fractographic examination (Photo 1 (b)) on a specimen that interrupted the test at the shear strain of about 30% (TP #1 in Table 1), then fractured at -196°C in a tensile mode, reveals that the entire fractured surface shows cleavage fracture associated with post-test failure at -196°C. And, it is also seen that no crack initiation perpendicular to the principal stress direction (45° inclination to fractured surface) during the torsion test has taken place at about 30% shear strain.

The stress state of a material subjected to three-dimensional tensile stress can be reduced to a two-dimensional stress state if the third tensile stress is subtracted from the three stress components, if the fact that a moderate hydrostatic stress does not affect the plastic deformation is taken into consideration. In the elastic stress field, the combination of a tensile stress in a coordinate axis and a compression stress in another coordinate axis normal to the first axis causes a shear stress on a plane inclined 45° to the two axes. Thus, the torsion test exactly simulates a test under a combined (tri-axial) stress field. Therefore, the results obtained by the torsion tests prove that heavy-section ductile cast iron has sufficient ductility even under tri-axial stress state condition.

FRACTURE TOUGHNESS TEST

Two kinds of fracture toughness tests were carried out. One is the test to measure the initiation fracture toughness and another is to obtain the arrest fracture toughness. The initiation toughness tests were performed in conformity with ASTM E399 test standards, Annex 7 (ASTM 1990) under wide range of temperatures and rapid loading conditions. The stress intensity factor rates dK/dt were selected as greater than 300MPa$\sqrt{m}$/s to represent the strain rate in a 100 ton class cask with impact limiters suffered from the 9-meter drop test. For the case of linear elastic break, critical stress intensity factor $K_{IC,R}$ at the onset of brittle fracture was obtained. The subscript R denotes the rapid loading. For the case of elastic-plastic failure, the initiation of ductile tearing prior to the brittle instability was determined either by an electrical potential drop technique (Lowes et al. 1971) or key-curve method (Ernst et al. 1979). The J-integral value associated with the ductile crack initiation was first obtained in conformity with ASTM E813 test standard (ASTM 1989), then it was converted to critical stress intensity factor and denoted as $K_{IC,R}^{JI}$.

The arrest toughness tests were carried out in conformity with ASTM E1221 test method (ASTM 1988), except that the specimen had a temperature gradient. One side of the specimen (initiation site) was cooled down by liquid nitrogen fumes, and the opposite side was heated up by a burner to obtain a steep temperature gradient. Fig. 2 shows an example of temperature distribution in a specimen and the locations where brittle fracture initiated and arrested. Using the displacements and crack length at the onset and the arrest of fracture, the arrest fracture toughness was calculated according to equation described in ASTM E1221 and denoted as K_{Ia}.

The results (model cask S: circles, model cask H: triangular, prototypic cask: rectangular marks) are shown in Fig. 3 as a function of temperature. The valid initiation toughness $K_{IC,R}$, the ductile tearing toughness $K_{IC,R}^{JI}$

and the arrest toughness K_{Ia} are shown by solid, open and double marks, respectively. The model cask H and the prototypic cask have higher fracture toughness than those of the model cask S, since the chemistries and heat treatments were modified from those of the model cask S. It is also seen in Fig. 3 that the temperature region above 0°C is upper-shelf for fracture toughness, since the fracture mode showed complete ductile fashion, while it showed a mixture of ductile and brittle failure below 0°C. Thus, the lower bound fracture toughness trend curve for the model cask S,

$$K_{IC,R}^{LB}\ [MPa\sqrt{m}] = \begin{cases} 110 & \text{for } T \geq 0°C \\ 24.5+1.334\exp[0.026(T°C+160)] & \text{for } T<0°C \end{cases} \quad (2)$$

and for the model cask H and the prototypic cask,

$$K_{IC,R}^{LB}\ [MPa\sqrt{m}] = \begin{cases} 133 & \text{for } T \geq 0°C \\ 48.1+1.334\exp[0.026(T°C+160)] & \text{for } T<0°C \end{cases} \quad (3)$$

are determined as equations (2) and (3), respectively (Urabe and Harada 1989). In Fig. 3, the K_{IR} curve for reactor pressure vessel steels described in Appendix G of ASME B & PV Code is also drawn, assuming the nil-ductility transition temperature (T_{NDT}) for the pressure vessel steels is -45°C, the same T_{NDT} as the model cask H (Urabe and Harada 1989). The results obtained by the fracture toughness tests shows that ductile cast iron has excellent fracture toughness at the lowest service temperature (-40°C) and high loading rate conditions.

SAFETY ASSESSMENT OF DCI CASK

For instance, Notification 501 issued by the Ministry of International Trade and Industry (MITI) or Boiler and Pressure Vessel Code by the American Society for Mechanical Engineers (ASME) describes safety assessment methods of nuclear power plant components, providing that the materials have possession of enough ductility even under tri-axial (combined) stress states at the lowest service temperature. The results obtained by the torsion tests proved that heavy-section ductile cast iron for casks is ductile at the lowest service temperature of -40°C. Thus, the same safety assessment methodology of MITI Notification or ASME B & PV Code can be applied to analyze the safety assessment of the DCI casks.

The structural integrity of casks should be assured so that brittle failure never takes place even if a crack-like flaw of fairly large size associated with the detection sensitivity of non-destructive tests (NDT) is postulated in the cask. Thus, a linear elastic fracture mechanics approach would be appropriate to make the safety assessment of casks. The ASME B & PV Code, Section III, Appendix G or The MITI Notification 501 requires for the nuclear power plant components that the stress intensity factor K_I multiplied by a factor of safety, 2, should be less than the reference fracture toughness K_{IR} that envelopes the minimum values of static, dynamic and arrest fracture toughness. Thus, once the stress due to mechanical tests required by the IAEA regulations and a postulated crack size associated with NDT are determined, the safety analysis can be made by the same methodology. However, the stress arising in a cask due to the hypothetical accidents must be analyzed in the details, since the section thickness of the cask is mainly determined by the γ-ray shielding efficiency, while it is essentially determined to retain internal pressure for the case of reactor pressure vessels.

The forces expected to be directed to a cask include:

1) static force by external mechanical force,
2) static force by self weight,
3) impact force by external mechanical force, and
4) impact force by self-weight (free drop test)

are considered. Those forces are illustrated in Fig. 4, and the stresses corresponding to each loading mode are obtained. Dependence of the stress on the section thickness t varies regarding the loading mode. For example, the stress due to static force by self weight is independent of t, while it is inversely proportional to t for the case of free drop test.

On the other hand, ASME Code or MITI Notification requires use of a postulated surface crack of 1 by 6 aspect ratio to calculate the applied stress intensity factor. And the depth of the surface crack must be proportional to

the section thickness of component. However, the analysis on the round robin tests by ultrasonic investigation performed to clarify the detection sensitivity on heavy-section DCI blocks revealed that the detection sensitivity is independent of the section thickness and a constant value of 20mm (Imaeda et al. 1992). Therefore, the dependence of stress intensity factor on the section thickness t is calculated under the assumptions that

1) $a_{p1} \propto t$: postulated crack size is proportional to the section thickness (ASME and MITI), and

2) a_{p2}=const. : postulated crack size is a constant value (results of RRT).

The results are also given in Fig. 4. The stress intensity factor of the cask is found to be a constant or decreasing function of the section thickness, except for the case of static force by self weight (this stress mode is less important, though). Therefore, the requirement of fracture toughness for the cask material should be constant or a decreasing function of the section thickness.

Assuming the postulated crack size is 20mm and the stress is 100MPa ($=\sigma_Y/2$), the stress intensity factor K_I is obtained as 25MPa$\sqrt{m}$. On the other hand, the reference fracture toughness of K_{IR}^{DCI} at -40°C assumed by equation (2) is 55MPa$\sqrt{m}$. This result means that the DCI cask never fails even if suffering from the hypothetical accidents required by the IAEA regulations. The ratio of K_{IR}/K_I, the factor of safety, is more than 2.

CONCLUDING REMARKS

The results of torsion tests conducted at low temperatures revealed that ductile cast iron has sufficient ductility even under the tri-axial stress state condition. The results by fracture toughness tests performed at high loading rates also showed that ductile cast iron has excellent fracture toughness under the lowest service temperature.

Analyses of the safety assessment on the cask were carried out based on a linear elastic fracture mechanics approach. Using the results obtained by the tests, it was shown that casks produced by ductile cast iron have enough ductility and toughness to preclude the brittle failure under the hypothetical accident conditions described in the IAEA regulations.

REFERENCES

ASME Code, Boiler and Pressure Vessel Code, Sect. III, "Rules for Construction of Nuclear Power Plant Component," Appendix G, "Protection against Non-Ductile Failure", (1991)

ASTM Standard, "Specification for Ferritic Ductile Iron Castings Suitable for Low Temperature Service", Designation A874 (1989)

ASTM Standard, "Standard Test Method for Plane-Strain Fracture Toughness of Metallic Materials", Designation E399 (1990)

ASTM Standard, "Standard Test Method for J_{IC}, A Measure of Fracture Toughness", Designation E813 (1989)

ASTM Standard, "Standard Test Method for Determining Plane-Strain Crack Arrest Fracture Toughness", Designation E1221 (1988)

Ernst, H. A., Paris, P. C., Rossow, M. and Hutchinson, J. W., "Analysis of Load-Displacement Relationship to Determine J-R Curve and Tearing Instability Material Properties", Fracture Mechanics, ASTM STP 677, Smith, C. W., Ed., ASTM (1979), pp. 581-599

Harada, Y. and Urabe, N., "Design and Fabrication of NKK Dry Transportation and Storage Cask", Proceedings of the Joint International Waste Management Conference, Vol. 2, (1989), pp. 77-82

IAEA Safety Standards No. 6, "Regulations for the Safe Transport of Radioactive Materials", IAEA, (1985)

Imaeda, H., Arai, T. and Onchi, T., "On A Round Robin Test of Nodular Graphite Iron Blocks by Ultrasonic Testing", Central Research Institute for Electrical Power Industry, Rep. No. T90059 (1991)

JIS Standard, "Heavy-Walled Ferritic Spheroidal Graphite Iron Castings for Low Temperature Service", Designation G 5504 (1992)

Lowes, J. M. and Fearnehough, G. D., "The Detection of Slow Crack Growth in Crack Opening Displacement Specimens Using an Electrical Potential Method", Engineering Fracture Mechanics, Vol. 3 (1971)

Urabe, N. and Harada, Y., "Fracture Toughness of Heavy-Section Ductile Iron Castings and Safety Assurance Method of DCI Casks", NKK Technical Report, Vol. 125 (1989), pp. 77-84

Urabe, N. and Harada, Y., "Fracture Toughness of Heavy Section Ductile Iron Castings and Safety Assessment of Cast Casks", Proceedings of the 9th International Symposium on the Packaging and Transportation of Radio Active Materials", Vol., 2 (1989), pp. 743-752

Yamase, O. et al, "BOF Technic based on Pre-Treatment Hot Metal", NKK Technical Report, Vol., 118 (1987), pp. 1-8

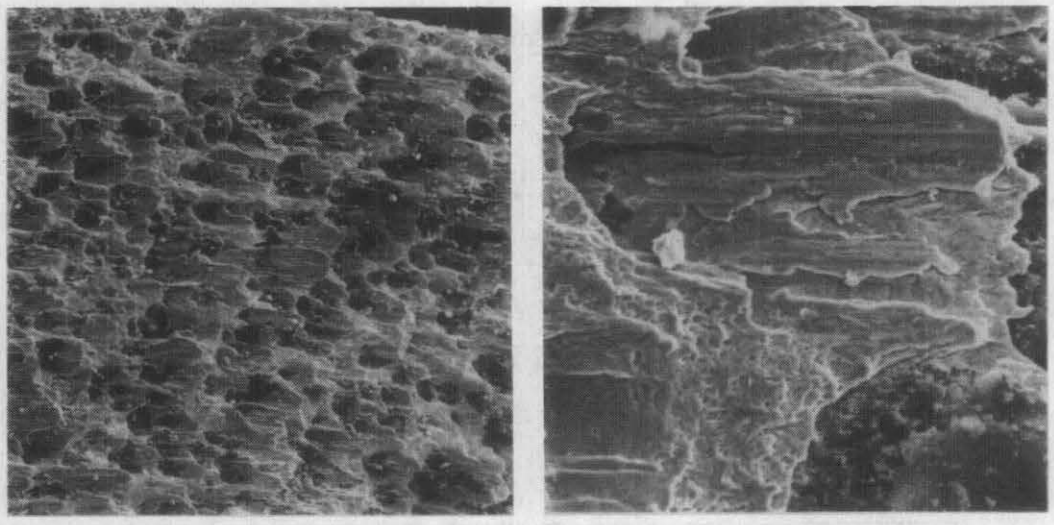

(a)

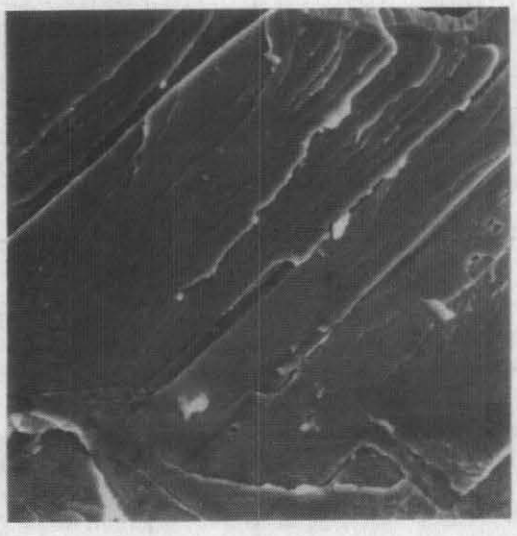

(b)

Photo 1 Examples of fractographic examination

Table 1 Results of torsion tests

TP#	T(℃)	$d\gamma/dt$(1/s)	$\tau_{0.3}$(N/mm²)	ϕ_B(deg)	γ_B(%)
1*	18	2.18×10^{-4}	156.6	349→	30.4→
2	18	3.32×10^{-4}	158.8	1155	100.8
3	18	3.58×10^{-3}	161.7	1174	102.4
4	18	3.32×10^{-3}	165.6	956	83.4
7	-40	2.71×10^{-4}	182.3	675	58.9
8	-40	2.36×10^{-4}	176.4	1031	90.0
9	-40	3.41×10^{-3}	191.1	741	64.6
10	-40	3.27×10^{-3}	189.1	956	83.5

* Interrupted at γ=30%, then fractured at -196℃

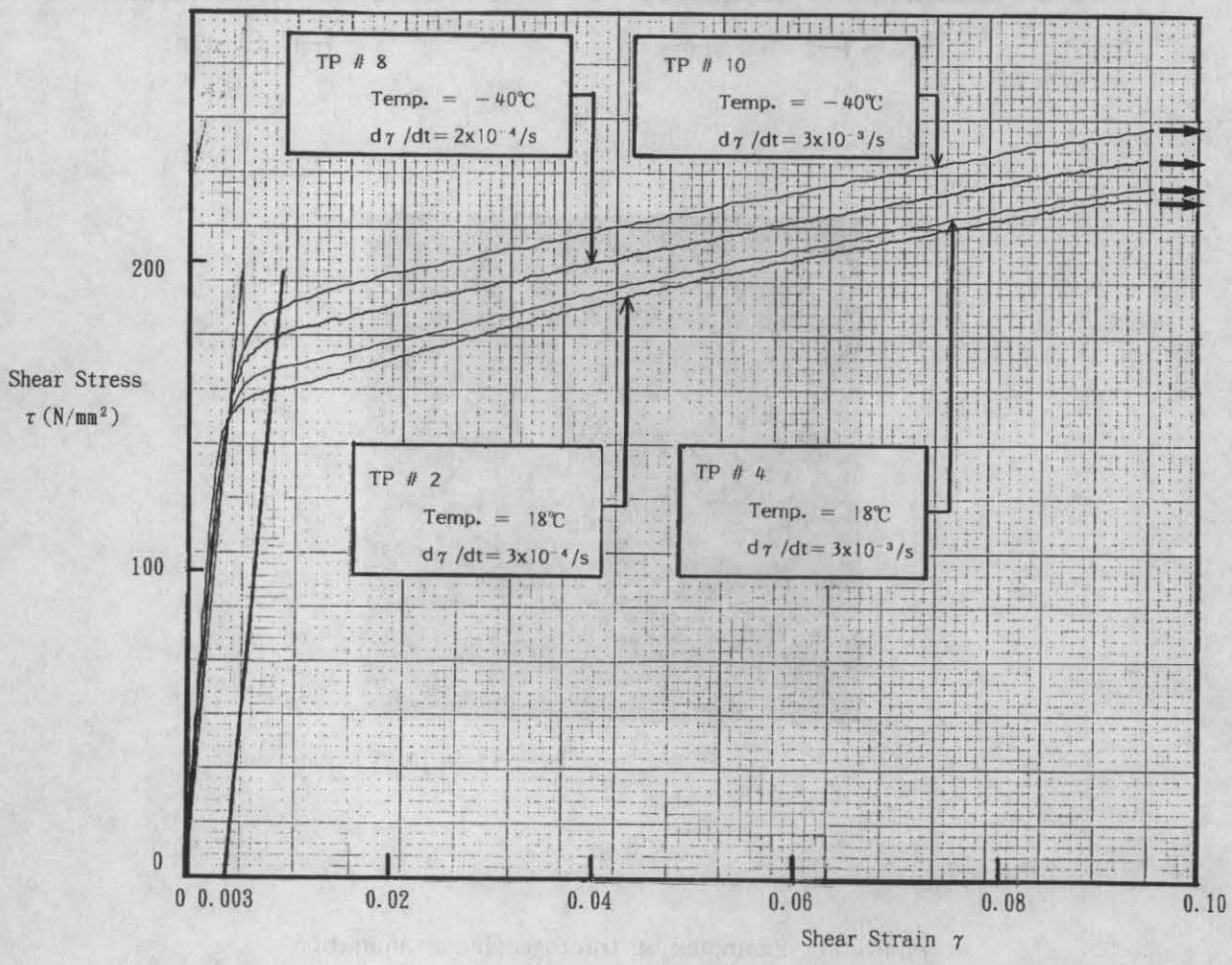

Fig 1 Examples of shear stress and shear strain record

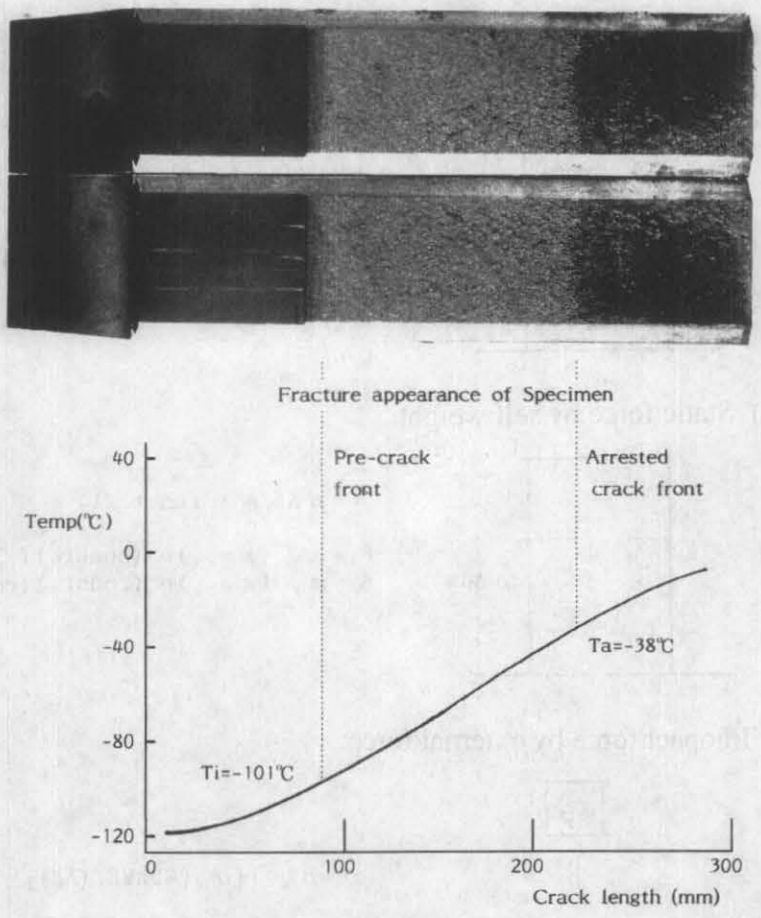

Fig. 2 An example of temperature distribution and crack arrest location

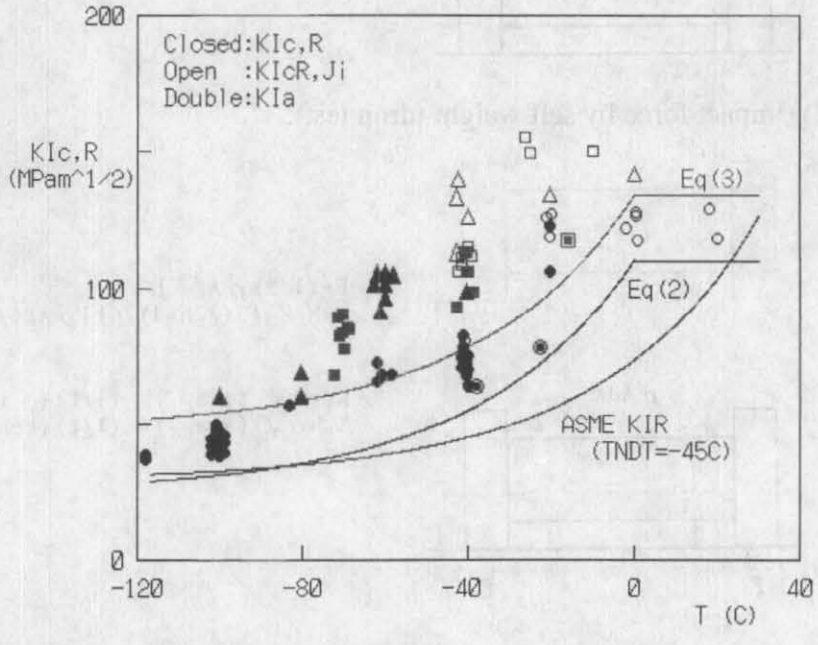

Fig. 3 Fracture toughness of DCI and estimation of lower bound curves
(Circles:Model S, Triangles:Model H, Rectangulars:Prototypic cask)

1) Static force by external force:

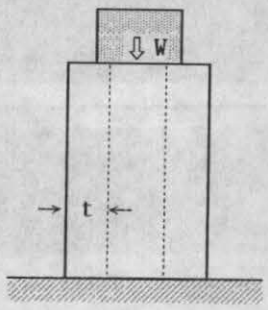

$\sigma = W/(\text{Sect. Area}) \propto 1/t$

$K_I = \sigma \sqrt{(\pi a_{P1})} \propto (1/t)(\sqrt{t}) \propto 1/\sqrt{t}$
$K_I = \sigma \sqrt{(\pi a_{P2})} \propto (1/t)(\text{const.}) \propto 1/t$

2) Static force by self weight:

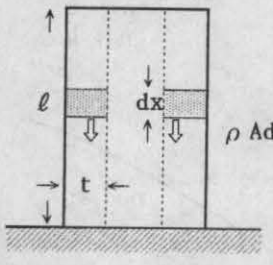

$\sigma = \rho A\ell/A \neq \text{funct.}(t)$

$K_I = \sigma \sqrt{(\pi a_{P1})} \propto (\text{const.})(\sqrt{t}) \propto \sqrt{t}$
$K_I = \sigma \sqrt{(\pi a_{P2})} \propto (\text{const.})(\text{const.}) \propto \text{const.}$

3) Imopact force by external force:

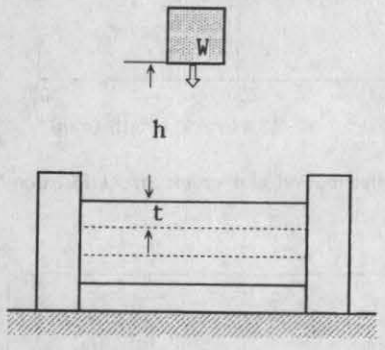

$\sigma = \sigma_{st} + [\sigma_{st} + 2hWE/(A\ell)]^{1/2} \propto 1/\sqrt{t}$

$K_I = \sigma \sqrt{(\pi a_{P1})} \propto (1/\sqrt{t})(\sqrt{t}) = \text{const.}$
$K_I = \sigma \sqrt{(\pi a_{P2})} \propto (1/\sqrt{t})(\text{const.}) \propto 1/\sqrt{t}$

4) Impact force by self weight (drop test):

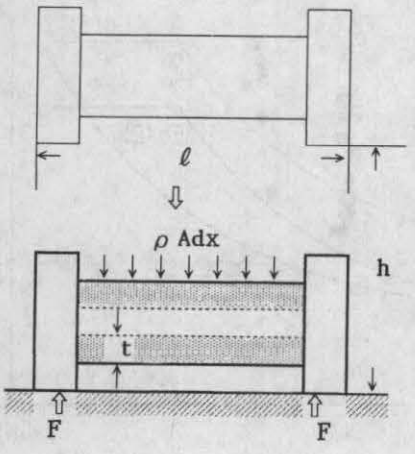

$F = (1/2)\rho A\ell\sqrt{h}$
$\sigma = M/Z = [3(\sqrt{h}-1)/4][\rho A\ell^2/At] \propto 1/t$

$K_I = \sigma \sqrt{(\pi a_{P1})} \propto (1/t)(\sqrt{t}) \propto 1/\sqrt{t}$
$K_I = \sigma \sqrt{(\pi a_{P2})} \propto (1/t)(\text{const.}) \propto 1/t$

Fig. 4 Applied stress intensity factor